Article

A Dual-Response Fluorescent Probe for the Detection of Viscosity and H2S and Its application in Studying Their Cross-Talk Influence in Mitochondria

Song-Jiao Li, Yongfei Li, Hong-Wen Liu, Dong-Ye Zhou, Wen-Li Jiang, Juan Ou-Yang, and Chun-Yan Li

Anal. Chem., **Just Accepted Manuscript** • DOI: 10.1021/acs.analchem.8b02068 • Publication Date (Web): 05 Jul 2018

A Dual-Response Fluorescent Probe for the Detection of Viscosity and H_2S and Its application in Studying Their Cross-Talk Influence in Mitochondria

Song-Jiao Li,[†] Yong-Fei Li,*[,†,‡] Hong-Wen Liu,[†] Dong-Ye Zhou,[†] Wen-Li Jiang,[†] Juan Ou-Yang,[†] Chun-Yan Li*[,†,§]

[†]Key Laboratory for Green Organic Synthesis and Application of Hunan Province, Key Laboratory of Environmentally Friendly Chemistry and Applications of Ministry of Education, College of Chemistry, Xiangtan University, Xiangtan, 411105, PR China.

[‡]College of Chemical Engineering, Xiangtan University, Xiangtan, 411105, PR China.

[§]State Key Laboratory of Chemo/Biosensing and Chemometrics, College of Chemistry & Chemical Engineering, Hunan University, Changsha, 410082, PR China.

*Corresponding Author. E-mail: lichunyan79@sina.com (Chun-Yan Li), liyongfei@xtu.edu.cn (Yong-Fei Li).

ABSTRACT: Intracellular viscosity is an essential micro-environmental parameter and H_2S is a critical gaseous signaling molecule, which are both related to various physiological processes. It is reported that the change of viscosity and an imbalance of H_2S production in the mitochondria are both associated with over-expression of amyloid betapeptide (Aβ), which is thought to play a central role in the pathogenesis of Alzheimer's disease (AD). However, to our best knowledge, no fluorescent probe is found for dual detection of mitochondrial viscosity and H_2S. Herein, a dual-response fluorescent probe (Mito-VS) is designed and synthesized to monitor the level of viscosity and H_2S, respectively. Mito-VS itself is nonfluorescent due to a free intramolecular rotation between dimethylaniline and pyridine. After the increase of viscosity, the rotation is prohibited and an intense red fluorescence is released. While, upon the addition of H_2S, the probe can react with H_2S to form compound **3** and a strong green fluorescence can be observed. Moreover, the probe possesses a good mitochondrion-targeting ability and is applied for imaging the change of viscosity on red channel and visualizing the variation of exogenous and endogenous H_2S concentration on green channel in mitochondria. Most importantly, the probe is capable of studying cross-talk influence of viscosity and H_2S in mitochondria, which is very beneficial for knowing the pathogenesis of AD.

Intracellular viscosity, an essential micro-environmental parameter, plays an important role in the transportation of signals as well as the interactions between biomolecules.[1-3] Mitochondria, known as power house, play critical roles in cellular viability and the overall health.[4] The viscosity of mitochondria reflects the status and function of the organelle.[5] Hydrogen sulfide (H_2S) is a critical signaling gasotransmitter, has been recognized to mediate a wide range of physiological processes such as vasodilation, angiogenesis, apoptosis, inflammation, and neuromodulation.[6-10] H_2S biology is associated with certain organelles like mitochondria.[11,12] And mitochondrial H_2S has been shown to exert protective effects in oxidative stress resulting in dysfunction and cell death.[13-15] In particular, studies have indicated that both the change of viscosity and abnormal levels of H_2S in the mitochondria are both related to amyloid betapeptide (Aβ) accumulation, which is considered to be a key pathogenic factor in sporadic Alzheimer's disease (AD).[16-19] AD is a progressive disorder that leads to dementia and affects approximately 10% of the population older than 65 years of age. Memory loss is the first sign of cognitive impairment followed by behavioral disturbances.[20] And understanding pathogenesis of AD will provide a basis for early therapeutic interventions and thus delaying AD progression in elderly individuals. Therefore, there is a intense need to develop methods for dual detection of mitochondrial viscosity and H_2S in order to better know the pathogenesis of AD.

Fluorescent probes together with microscopy have become an effective tool due to their sensitivity, visualization, high spatial and temporal resolution.[21-29] To date, many well-designed fluorescent probes have been reported for imaging mitochondrial viscosity.[30-32] Moreover, several fluorescent probes for detection and visualization of H_2S in mitochondria have been successfully developed.[33-36] However, no report describing a single fluorescence probe capable of dual detection and imaging of viscosity and H_2S can be found by us. A single probe with different spectral responses towards multiple analytes can overcome the difficulties including uneven probe loading and interference of photo-bleaching encountered by simply combining of several fluorescent probes in one system.[37] To date, many excellent probes have been elaborated for multiple analytes using a single fluorescent probe.[38-46] Thus, developing a single fluorescent probe that can simultaneous detection and imaging of viscosity and H_2S in mitochondria is urgently needed.

Herein, we design and synthesize a dual-response fluorescent probe (Mito-VS) to monitor the level of viscosity and H_2S (Scheme 1). Mito-VS itself is nonfluorescent because there is a free intramolecular rotation between dimethylaniline and pyridine and thus twisting intramolecular charge transfer (TICT) state is observed. On the one hand, with viscosity increasing, the rotation is restricted and a strong red fluorescence is released. On the other hand, after the addition of H_2S, the azide in the probe is reduced to amine, followed by elimination reaction to give compound **3**. A remarkable green fluorescence signal can be monitored due to the presence of intramolecular charge transfer (ICT) state in compound **3**. In addition, Mito-VS, a positive charged molecule, possesses a good mitochondrion-targeting ability and is applied for imaging the change of viscosity and H_2S concentration in mitochondria on the red channel and green channel, respectively. Particularly, the probe is capable of investigating cross-talk influence of viscosity and H_2S in mitochondria, which will provide a power tool for understanding pathogenesis of AD.

Scheme 1. The Design for Probe Mito-VS.

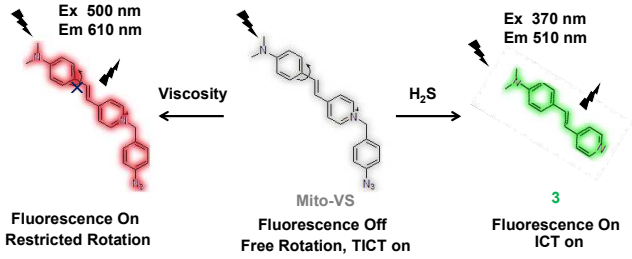

EXPERIMENTAL SECTION

Reagents. 4-aminobenzylalcohol, sodium nitrite ($NaNO_2$), sodium azide (NaN_3), phosphorus tribromide (PBr_3), 4-bromo-N,N-dimethylaniline, 4-vinylpyridine, palladium acetate, and tri-*o*-tolylphosphine were purchased from Macklin and used without further purification. All other chemicals and reagents were obtained from Shanghai Chemical Reagent Corporation and used without further purification.

Apparatus. ^1H and ^{13}C NMR spectra were recorded on a Bruker Avance II spectrometer (Germany) at 400 MHz or at 100 MHz (TMS as internal standard). Mass spectra (MS) were measured with a Bruker Autoflex MALDI-TOF MS spectrometer (Germany). Element analysis was conducted on Perkin Elmer 2400 elemental analyzer (USA). All fluorescence measurements were taken on a Perkin Elmer LS-55 fluorescence spectrometer (USA). The viscosity was measured with a NDJ-7 rotational viscometer (China). UV-vis absorption spectra were recorded with a Perkin Elmer Lambda 25 spectrophotometer (USA). Fluorescence images of HeLa cells were obtained using an Olympus FV1000 laser confocal microscope (Japan).

Synthesis. A synthetic route for compound Mito-VS from commercially available compounds was provided and depicted in Scheme 2.

Compound 1*:* To a solution of $NaNO_2$ (0.52 g, 7.5 mmol) in water (15 mL), 4-aminobenzylalcohol (0.62 g, 5.0 mmol) dissolved in HCl (6.0 M, 5 mL) was added dropwise at 0 °C. The reaction was stirred at this temperature for 30 min and then NaN_3 (1.3 g, 20 mmol) dissolved in water (15 mL) was added dropwise. The reaction mixture was stirred at room temperature for another 2 h. After extraction with ether three times, the organic phase was washed sequentially with saturated $NaHCO_3$ solution to obtain a yellow oil product. Yield: 0.63 g (85 %). ^1H NMR (400 MHz, $CDCl_3$) δ (ppm) 7.20 (d, J = 8.0 Hz, 2H), 6.90 (d, J = 8.0 Hz, 2H), 4.47 (s, 2H). MS $[M+H]^+$ calcd. 150.1, found 150.1.

Compound 2*:* Compund 1 (0.38 g, 2.5 mmol) was dissolved in trichloromethane ($CHCl_3$, 20 mL) under N_2 atmosphere, and PBr_3 (0.80 g, 3.0 mmol) was added dropwise at room temperature. The reaction mixture was then stirred at room temperature overnight. After the completion of reaction, the organic phase was washed sequentially with saturated $NaHCO_3$ solution to obtain a yellow oil product. Yield: 0.51 g (96 %). ^1HNMR (400 MHz, $CDCl_3$) δ (ppm) 7.37 (d, J = 8.0 Hz, 2H), 6.91 (d, J = 8.0 Hz, 2H), 4.48 (s, 2H). MS (TOF): $[M+H]^+$ calcd. 212.0, found 212.0.

Compound 3: 4-Bromo-N,N-dimethylaniline (2.0 g, 10 mmol), 4-vinylpyridine (4.0 mL, 12 mmol), palladium acetate (0.02 g, 0.1 mmol) and tri-*o*-tolylphosphine (0.06 g, 0.2 mmol) were dissolved in triethylamine (Et_3N, 30 mL). The mixture was refluxed overnight and cooled to room temperature. After the removal of solvent under reduced pressure, the residue was purified by column chromatography with hexane/CH_2Cl_2 = 1:25 as the eluent to obtain a yellow solid product. Yield: 1.8 g (80 %). ^1H NMR (400 MHz, $CDCl_3$, Figure S1) δ (ppm) 8.53 (d, J = 6.0 Hz, 2H), 7.45 (d, J = 8.8 Hz, 2H), 7.33 (d, J = 6.0 Hz, 2H), 7.26 (d, J = 16.0 Hz, 2H), 6.82 (d, J = 16.0 Hz, 1H), 6.73 (d, J = 8.0 Hz, 1H), 3.03 (s, 6H). ^{13}C NMR (100 MHz, $CDCl_3$, Figure S2) δ (ppm) 150.8, 150.0, 145.6, 133.4, 128.3, 124.3, 121.2, 120.4, 112.2, 40.3. MS (TOF, Figure S3): $[M+H]^+$ calcd. 225.1, found 225.2.

Scheme 2. Synthetic Route for Mito-VS.

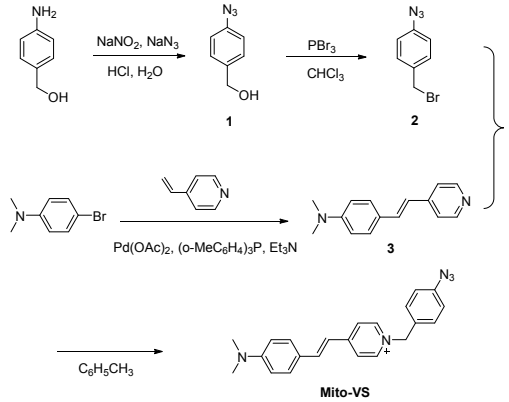

Compound Mito-VS: Compound **2** (0.32 g, 1.5 mmol) and compound **3** (0.34 g, 1.5 mmol) were dissolved in toluene ($C_6H_5CH_3$, 20 mL). The mixture was refluxed for 12 h. After the removal of solvent under reduced pressure, and the residue was purified by column chromatography with CH_2Cl_2/CH_3CH_2OH = 20:1 as the eluent to obtain a reddish solid product. Yield: 0.48 g (88%). ^1H NMR (400 MHz, $CDCl_3$, Figure S4) δ (ppm) 9.07 (d, J = 6.8 Hz, 2H), 7.75 (d, J = 7.2 Hz, 2H), 7.68 (d, J = 8.4 Hz, 2H), 7.55 (d, J = 16.0 Hz, 1H), 7.51 (d, J = 8.8 Hz, 2H), 7.00 (d, J = 8.4 Hz, 2H), 6.79 (d, J = 16 Hz, 1H), 6.68 (d, J = 8.8 Hz, 2H), 5.99 (s, 6H). ^{13}C NMR (100 MHz, $CDCl_3$, Figure S5) δ (ppm) 154.4, 152.5, 143.3, 141.6, 131.2, 130.8, 130.1, 122.5, 122.2, 120.0, 116.2, 112.0, 61.9, 40.1. MS (TOF, Figure S6): $[M]^+$ calcd. 356.5, found 356.3. Elem. anal. (%) calcd for $C_{22}H_{22}N_5$: C, 74.13; H, 6.22; N, 19.65. Found: C, 74.06; H, 6.23; N, 19.68.

Viscosity Analysis in Vitro. The solutions for viscosity were prepared by mixing ethanol and glycerol in different proportions. The measurements were carried out with a viscometer and each viscosity value was recorded. The solutions of probe Mito-VS in different viscosity were prepared by adding the stock solution of Mito-VS (10.0 mM, 10.0 μL) to ethanol-glycerol solution (10.0 mL) to obtain the final concentration of Mito-VS (10.0 μM). These solutions were sonicated for 10 min to eliminate air bubbles and standing for 1 hour at a constant temperature. And then the fluorescence spectra were recorded at the excitation of 500 nm with the excitation and emission slit widths set at 5 nm and 5 nm, respectively. The relationship between the fluorescence emission intensity of the probe and the viscosity of the solvent is well expressed by Forster-Hoffmann equation as following:

$$\text{Log } (I_f) = c + x \text{ Log } \eta$$

Where I_f is the fluorescence intensity, η is the viscosity of solution, x and c are constant.

H_2S Analysis in Vitro. Na_2S was used as H_2S source and its stock solution was prepared by dissolving Na_2S in phosphate-buffered saline (PBS, pH 7.4) solution. And the Na_2S stock solution was further diluted to 1-100 μM stepwise. The solutions of probe Mito-VS with H_2S were prepared by adding the stock solution of Mito-VS (10.0 mM, 10.0 μL) to Na_2S solution (10.0 mL) to obtain the final concentration of Mito-VS (10.0 μM). The fluorescence spectra was then measured at the excitation of 370 nm with the excitation and emission slit widths set at 5 nm and 5 nm, respectively.

Cell Culture and Fluorescence Imaging. The living HeLa cells were obtained from the Biomedical Engineering Center of Hunan University (Changsha, China). HeLa cells were grown in Dulbecco's Modified Eagle Medium (DMEM) supplemented with 10 % Fetal Bovine Serum (FBS) in an atmosphere of 5 % CO_2 and 95 % air at 37 °C. And then cells were plated on 35 mm culture dish and allowed to adhere for 24 hours. Moreover, all the cells during the experimental process were cultured at 37 °C and washed three times with PBS solution (pH 7.4) prior to fluorescence imaging. Fluorescence imaging was recorded by confocal fluorescence microscope.

RESULTS AND DISCUSSION

Spectroscopic Response of Probe Mito-VS to Viscosity. The fluorescent response of probe Mito-VS to various ethanol-glycerol solutions with different levels of viscosity was first investigated. As shown in Figure 1A, the probe shows almost no fluorescence in non-viscous solution and the fluorescence quantum yield of Mito-VS is less than 0.02. In contrast, a strong red fluorescence with emission peak at 610 nm is observed in high viscous solutions. With the increase of viscosity from 1.03 cP (100% ethanol) to 584.52 cP (5% ethanol and 95% glycerol), the fluorescence increases 10 folds with a quantum yield of 0.62. As shown in Figure 1B, a good linearity (R = 0.97) between $\log I_{610}$ and log(viscosity) in the range of 1.03 cP to 584.52 cP was obtained. Next, the absorption spectra of Mito-VS in ethanol-glycerol mixtures was measured. As shown in Figure S7, the absorption of Mito-VS at 500 nm changes little in solvents with different viscosity concomitant with a color change from orange to deep orange. Furthermore, the fluorescence spectra of the probe were measured at a variety of pH values. As shown in Figure S8, the fluorescence intensity of the probe at low or high viscosity do not change at all pH. All the results demonstrate the stability of probe Mito-VS for detecting the viscosity.

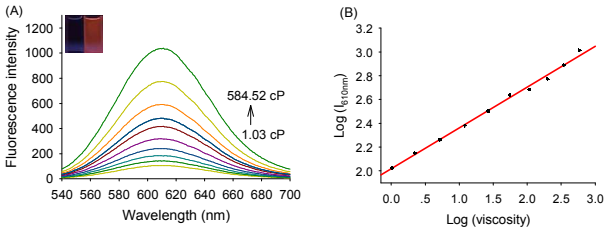

Figure 1. (A) Fluorescence spectra of Mito-VS (10 μM) in ethanol-glycerol solution with different viscosity (1.03-584.52 cP). Insert: the photographs of Mito-VS at low (left) and high (right) viscosity under a 365 nm UV lamp. (B) The curve is plotted with log (I_{610}) versus log (viscosity). λ_{ex} = 500 nm.

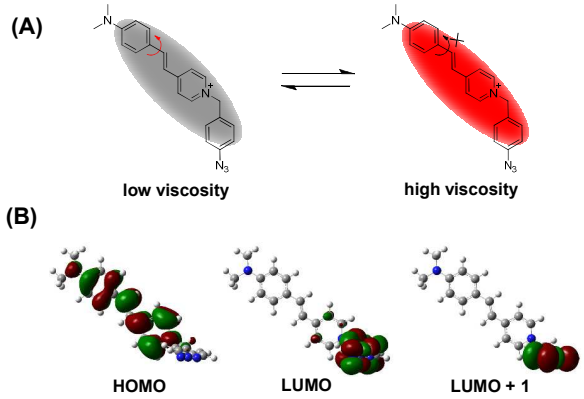

Figure 2. (A) The proposed response mechanism of Mito-VS towards viscosity. (B) The frontier molecular orbitals of Mito-VS acquired via DFT calculation.

Based on the evidence from spectroscopic data, a possible response mechanism of Mito-VS to viscosity was proposed (Figure 2A). In non-viscous or low-viscous environment, there is a free intramolecular rotation between dimethylaniline and pyridine, which results in very weak fluorescence by forming twisting intramolecular charge transfer (TICT) state. Whereas, at high-viscous environment, the rotation is restricted and a strong fluorescence is given, which hinder the formation of TICT state. The formation of TICT state in Mito-VS can be further proved via density functional theory (DFT) calculation with the B3LYP/6-311G method using the Gaussian 09 package (Figure 2B). DFT calculation displays that the photoexcitation of Mito-VS from S0 to S1 states mainly contains electron transitions from the highest occupied molecular orbital (HOMO) to both the lowest occupied molecular orbital (LUMO) and LUMO+1. The HOMO of Mito-VS is mainly positioned at dimethylaniline group, but the LUMO and LUMO+1 is mostly located on pyridine group. The frontier molecular orbital diagram imply that there is a strong charge transfer process in the excited state from dimethylaniline to pyridine group, which implied a typical TICT process. Based on the above discussion, it may be concluded that probe Mito-VS acts as an effective TICT-based fluorescent probe for viscosity.

Spectroscopic Response of Probe Mito-VS toward H_2S. The fluorescent response of probe Mito-VS with various concentrations of H_2S (Na_2S was used as H_2S source) in PBS solution was initially studied (Figure 3A). Free Mito-VS displays a very weak emission at 510 nm. Upon the addition of H_2S, a remarkable green fluorescence enhancement at 510 nm

is observed with high fluorescence quantum yield (Φ_f = 0.57). With the increase of H_2S concentration from 0.0 to 100.0 μM, the fluorescence of Mito-VS is enhanced 7 folds. As Figure 3B shows, the fluorescent intensity is found to be linearly proportional to H_2S concentration at the range of 0.5-100 μM. The detection limit ($3\sigma/k$) for H_2S was calculated to be 0.17 μM. Moreover, the UV-vis absorption spectra of Mito-VS with different concentrations of H_2S were recorded (Figure S9). The absorption peak at 500 nm decreases gradually and a new absorption peak at 370 nm arises with a color change from yellow to colorless. Next, the effect of pH on the fluorescence intensity of the probe in absence and presence of Na_2S was performed. As shown in Figure S10, the probe possesses good fluorescence response toward H_2S in the pH range of 6.0-11.0. The results show that the probe can be used under the physiological condition (pH 7.4), which is favorable for biological imaging. Furthermore, the selectivity of the probe for H_2S was evaluated. As shown in Figure 3C, when the potential interference species such as biothiols (Cys, Hcy, GSH), reactive sulphur species (SO_3^{2-}, $S_2O_3^{2-}$, SCN^-), reactive oxygen species (H_2O_2, $O_2^{\cdot-}$, ClO^-), reactive nitrogen species (NO, NO_2^-, NO_3^-) and metal ions (K^+, Na^+, Ca^{2+}) are tested, none of the species causes obvious fluorescence change. The above result suggests the high selectivity of Mito-VS toward H_2S. In addition, the fluorescence of Mito-VS at varied concentrations of H_2S was monitored with time (Figure 4D). In all cases, stable reading can be acquired in 30 min. Once the fluorescence intensity reaches a plateau, it stays relatively stable for the remainder of the measurement, indicating that the probe is photostable under irradiation. All the results indicate that probe Mito-VS has the ability to detect H_2S.

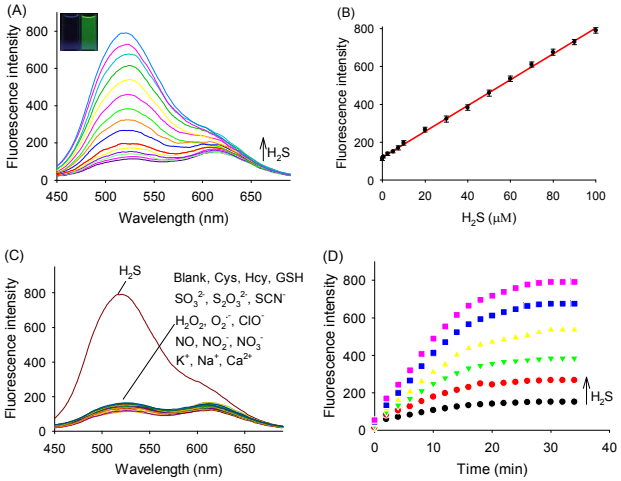

Figure 3. (A) Fluorescence spectra of Mito-VS (10 μM) in the presence of increasing amounts of Na_2S (0.0, 0.5, 2.5, 5.0, 7.5, 10.0, 20.0, 30.0, 40.0, 50.0, 60.0, 70.0, 80.0, 90.0, 100.0 μM) in PBS solution (pH 7.4). Insert: the photographs of Mito-VS in the absence (left) and presence (right) of Na_2S (100.0 μM) under a 365 nm UV lamp. (B) The curve is plotted with the fluorescence intensity versus H_2S concentrations. (C) Fluorescence response of Mito-VS (10 μM) toward H_2S (100 μM), GSH (1 mM) and other interference species (200 μM). (D) Time-dependent fluorescence intensity change of Mito-VS (10 μM) to varied concentrations of H_2S (5.0, 20.0, 40.0, 60.0, 80.0, 100.0 μM). λ_{ex} = 370 nm.

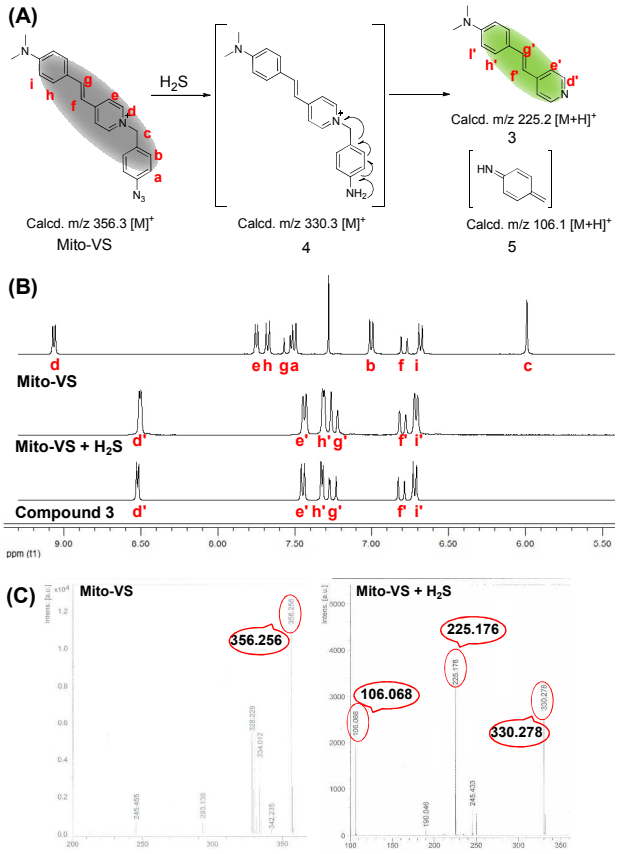

Figure 4. (A) The proposed response mechanism of Mito-VS towards H_2S. (B) Partial ^1H NMR analysis of Mito-VS, Mito-VS reacted with H_2S, compound **3** in $CDCl_3$. (C) Mass spectra of Mito-VS and Mito-VS reacted with H_2S.

Based on the evidence from the spectral data, the response mechanism of Mito-VS toward H_2S was proposed in Figure 4A. After adding H_2S, the azide in the probe is reduced to amine (compound **4**), followed by elimination reaction to give compound **3** and compound **5**. Owing to the presence of intramolecular charge transfer (ICT) state in compound **3**, a significant fluorescence signal can be monitored. To verify the response mechanism of Mito-VS to H_2S, ^1H NMR experiments were carried out (Figure 4B). Upon the addition of H_2S, the peaks at 7.51 and 7.00 for proton a and b of benzene and the peak at 5.99 for proton c of methylene disappear. Moreover, the notable chemical shift change of proton d, e, h, g are observed. The results indicate the production of new compound due to the reaction of Mito-VS and H_2S. And the main peaks of Mito-VS reacted with H_2S system match perfectly with compound **3**, displaying that the main reaction product of Mito-VS and H_2S is compound **3**. However, compound **4** is not identified presumably due to its instability. And compound **5** is also not found owing to the fact that it is prone to be attacked by water and various nucleophiles. However, it is interesting to see that the formation of compound **4** and compound **5** were well confirmed by the mass spectra (Figure 4C). Upon the addition of H_2S, the peak at m/z = 356.3 corresponding to Mito-VS vanishes, while the peaks at m/z = 106.1, m/z = 225.2 and m/z = 330.3 corresponding to compound **5**, compound **3** and compound **4** occur. All in all, these data provide strong support for the proposed mechanism.

Fluorescence Imaging of Viscosity in Living Cells. Before fluorescence imaging, the cytotoxicity of Mito-VS in living HeLa cells was evaluated by a standard MTT assay (Figure S11). The cell viability is kept above 90% even though the concentration of probe incubated in the cells is increased to 30 μM, indicating that the probe is applicable for imaging.

Next, the colocalization experiments was performed to evaluate the specific location of Mito-VS in mitochondria (Figure 5). Nystatin, a well-known ionophore that can induce mitochondrial viscosity alterations.[47] When the cells are incubated by nystatin and then incubated with Mito-VS, a clear red fluorescence image on red channel is observed (Figure 5a). Mito-Tracker Green (a commercially mitochondrial tracker) shows green fluorescence image on green channel (Figure 5b). The merged image indicates that the red fluorescence overlaps very well with the green fluorescence (Figure 5c). Figure 5d demonstrates bright-filed of the cells. And the intensity scatter plot displays good correlation with a high Pearson's colocalization coefficient of 0.91 (Figure 5e). The intensity profiles of the linear regions of interest across the cells also displays close synchronism (Figure 5f). In addition, a low Pearson's correlation coefficient of 0.33 is obtained from colocalization imaging of the cells treated with Mito-VS and Lyso Tracker Green (a commercially lysosomal tracker, Figure S12). These results clearly indicating that Mito-VS possesses good mitochondrion-targeting ability.

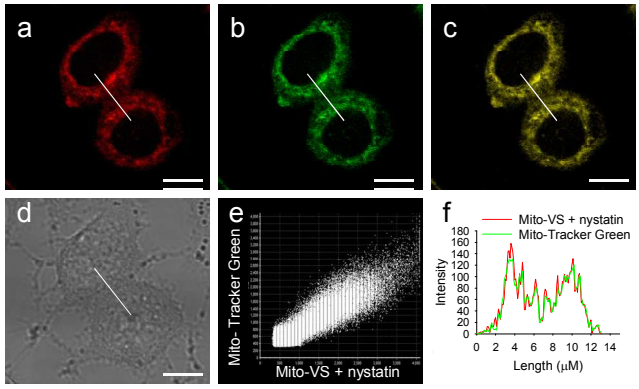

Figure 5. Colocalization imaging of HeLa cells staining with Mito-VS and Mito Tracker Green. (a) The cells were stained with nystatin (10 μM) for 30 min and then treated with Mito-VS (10 μM) for 30 min on red channel (λ_{ex} = 488 nm, λ_{em} = 545-645 nm). (b) The cells were stained with Mito Tracker Green (10 μM) for 30 min on green channel (λ_{ex} = 488 nm, λ_{em} = 495-525 nm). (c) Merged image of images (a) and (b). (d) Bright-field image. (e) Intensity scatter plot. (f) The intensity profile of linear regions of interest (ROI) across the cells. Scale bar: 10 μm.

With wonderful mitochondrion-targeting ability, Mito-VS was applied for mitochondrial viscosity imaging in HeLa cells (Figure 6). When the cells are treated by Mito-VS alone, a weak red fluorescence is observed (Figure 6a). However, when the cells are incubated by nystatin and then incubated with Mito-VS, about 3.8-fold fluorescence enhancement on red channel is displayed (Figure 6b). The fluorescence intensity of two groups of cells is calculated and the results are shown in Figure 6c. Above results suggest that Mito-VS can image viscosity in mitochondria very well.

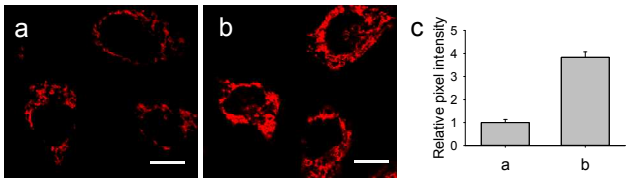

Figure 6. Fluorescence imaging of viscosity in HeLa cells. (a) The cells were stained with Mito-VS (10 μM) for 30 min. (b) The cells were treated with nystatin (10 μM) for 30 min and then stained with Mito-VS (10 μM) for 30 min. (c) The intensity of image a-b. Scale bar: 10 μm.

Fluorescence Imaging of H_2S in Living Cells. At first, the colocalization experiments was carried out to verify that Mito-VS can localize at mitochondria of living cells (Figure 7). The cells staining with Mito-VS and H_2S produce a bright green fluorescence on green channel (Figure 7a). The cells staining with Mito-Tracker Deep Red (a commercially mitochondria tracker) exhibit red fluorescence on red channel (Figure 7b). The merged image indicates that the green fluorescence overlaps very well with the red fluorescence (Figure 7c). Figure 7d demonstrates bright-filed of the cells. And the intensity scatter plot inhibits good correlation with a high Pearson's colocalization coefficient of 0.92 (Figure 7e). The intensity profiles of the linear regions of interest across the cells also indicate close synchronism (Figure 7f). In addition, a low Pearson's correlation coefficient of 0.42 is obtained from colocalization imaging of the cells staining with Mito-VS and Lyso Tracker Red (a commercially lysosomal tracker, Figure S13). These results demonstrate that, as designed, Mito-VS can specifically localize in mitochondria of living cells.

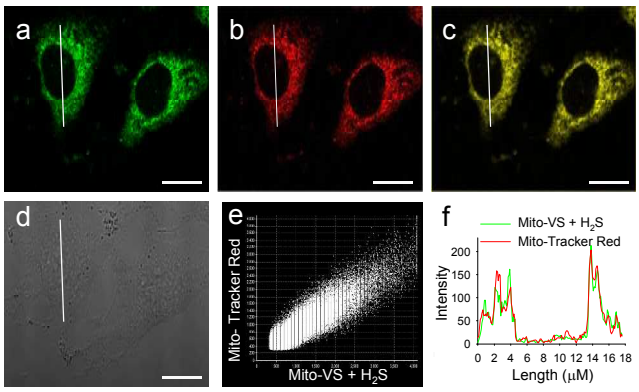

Figure 7. Colocalization imaging of HeLa cells staining with Mito-VS and Mito Tracker Deep Red. (a) The cells were stained with Mito-VS (10 μM) for 30 min and then treated with Na_2S (100 μM) for 30 min on green channel (λ_{ex} = 405 nm, λ_{em} = 425-525 nm). (b) The cells were stained with Mito Tracker Deep Red (10 μM) for 30 min on red channel (λ_{ex} = 640 nm, λ_{em} = 650-700 nm). (c) Merged image of images (a) and (b). (d) Bright-field image. (e) Intensity scatter plot. (f) The intensity profile of regions of interest (ROI) across the cells. Scale bar: 10 μm.

With excellent mitochondria-targeting ability, we set out to demonstrate its potential in cells imaging of exogenous and endogenous H_2S (Figure 8). As shown in Figure 8a, HeLa cells incubated only with Mito-VS exhibit very weak green fluorescence signal, implying intracellular basal level of H_2S. When the cells are pretreated with Mito-VS and then treated with Na_2S, an intense green fluorescence can be noticed (Figure 8b). And then the cells is pretreated with

propargylglycine (PAG), which is an inhibitor of H_2S production by cystathionine γ-lyase, the fluorescence signal decreases significantly (Figure 8c).[48] The results indicate that this probe can work well to monitor exogenous H_2S in living cells. Next, the efficacy of the probe for the detection of endogenous H_2S in HeLa cells were determined. When the cells are treated with Mito-VS and then incubated with Cys (Cys can induce the production of endogenous H_2S), a dramatic green fluorescence is found (Figure. 8d).[49,50] Moreover, the fluorescence intensity gradually enhances with time and reaches the maximum after 30 min (Figure S14). When the cells are stimulated with Cys, PAG, and then costained with Mito-VS, cellular fluorescence intensity is suppressed to some extent (Figure 8e). The fluorescence intensity of five groups of cells is calculated and the results are shown in Figure 8f. These imaging results strongly suggest that Mito-VS is suitable for visualization of both exogenous and endogenous H_2S in mitochondria of living cells.

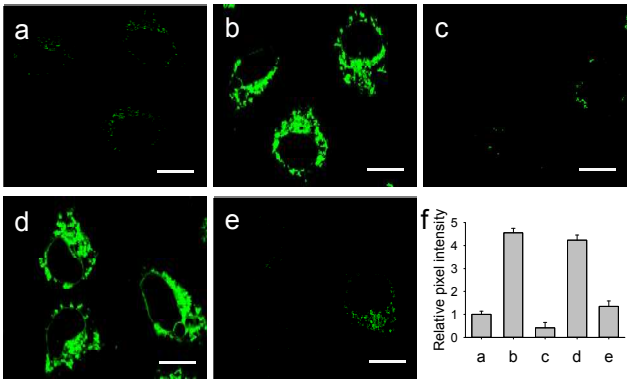

Figure 8. Fluorescence imaging of of H_2S in HeLa cells. (a) HeLa cells were stained with Mito-VS (10 μM) for 30 min. (b) HeLa cells were stained with Mito-VS (10 μM) for 30 min and then treated with Na_2S (100 μM) for 30 min (c) HeLa cells were preincubated with PAG (200 μM) for 30 min and incubated with Mito-VS (10 μM) for 30 min. (d) HeLa cells stimulated with Cys (100 μM) for 30 min and then costained with Mito-VS (10 μM) for 30 min. (e) HeLa cells stimulated with Cys (100 μM) for 30 min, PAG (200 μM) for 30 min, and then costained with Mito-VS (10 μM) for another 30 min. (f) The intensity of image a-e. Scale bar: 10 μm.

Cross-Talk Influence of Viscosity and H_2S in Living Cells. In virtue of the ability of Mito-VS in detecting viscosity and H_2S by dual channel, the cross-talk influence of them in cellular mitochondria were studied (Figure 9). When HeLa cells are treated by Mito-VS alone, a clear red fluorescence on red channel and a distinct green fluorescence on green channel are observed (Figure 9a and 9b). When the cells are incubated by nystatin and then with Mito-VS, a dramatic enhancement on red channel and a remarkable decrease on green channel are found (Figure 9c and 9d). This means that the increase of viscosity may lead to the decrease of H_2S in mitochondria. Moreover, when the cells are stimulated by Cys and then incubated with Mito-VS, a notable increase on green channel and a prominent decrease on red channel are discovered (Figure 9e and 9f). This displays that the increase of H_2S may result in the decrease of viscosity in mitochondria. The fluorescence intensity of three groups of cells on red channel and green channel is calculated, and the results are shown in Figure 9g and 9h. All these results indicate that the probe is capable of investigating cross-talk influence of viscosity and H_2S in mitochondria of living cells, which will provide a basis for knowing the pathogenesis of AD.

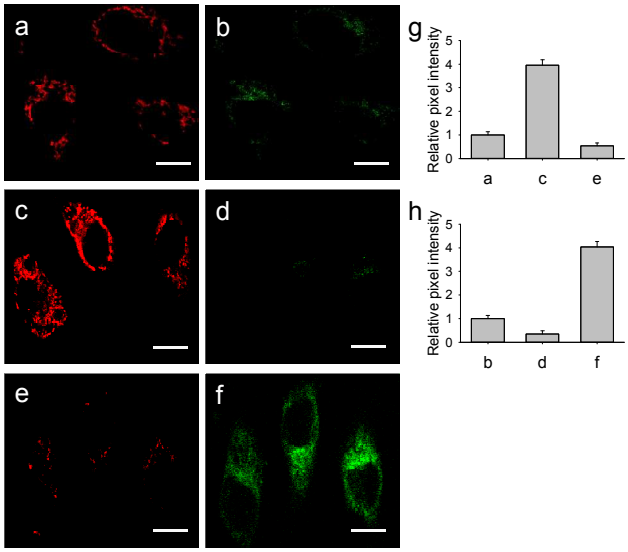

Figure 9. Fluorescence imaging of cross-talk influence of viscosity and H_2S in HeLa cells. The cells were stained with Mito-VS (10 μM) for 30 min on red channel (a) and green channel (b). The cells treated with nystatin (10 μM) and then stained with Mito-VS (10 μM) for 30 min on red channel (c) and green channel (d). The cells treated with Cys (100 μM) for 30 min and then stained with Mito-VS (10 μM) on red channel (e) and green channel (f). (g) The intensity of image a, c, e. (h) The intensity of image b, d, f. Scale bar: 10 μm.

CONCLUSIONS

In conclusion, a dual-response fluorescent probe (Mito-VS) is designed and synthesized for detecting viscosity and H_2S. With the increase of viscosity from 1.03 cP to 584.52 cP, the fluorescence of the probe is increased 10 folds. With the increase of H_2S concentration from 0.0 to 100.0 μM, the fluorescence of Mito-VS is enhanced 7 folds. Moreover, the probe possesses a good mitochondrion-targeting ability and high Pearson's colocalization coefficient (0.91 or 0.92). Furthermore, the probe is applied for imaging the change of viscosity induced by nystatin on red channel and visualizing exogenous and endogenous H_2S concentration on green channel in mitochondria. In addition, the probe is capable of studying cross-talk influence of viscosity and H_2S in mitochondria, which is very beneficial for knowing the pathogenesis of AD. It is anticipated that the probe become a powerful tool for early mitochondria targeted therapeutic interventions and thus delaying AD progression in elderly individuals in the future.

ASSOCIATED CONTENT

Supporting Information

The Supporting Information is available free of charge on the ACS Publications website.

^{1}H NMR, ^{13}C NMR and MS spectra, additional spectroscopic data, cell cytotoxicity and supplemental fluorescence images of cells.

AUTHOR INFORMATION

Corresponding Author

*E-mail: lichunyan79@sina.com (Chun-Yan Li).

*E-mail: liyongfei@xtu.edu.cn (Yong-Fei Li).

Notes

The authors declare no competing financial interest.

ACKNOWLEDGMENT

This work was supported by the National Natural Science Foundation of China (21775133), Hunan Provincial Natural Science Foundation of China (2015JJ6104, 2018JJ2385), State Key Laboratory of Chemo/Biosensing and Chemometrics Foundation (2015007), Scientific Research Fund of Hunan Provincial Education Department (15K125, 16B252), Hunan 2011 Collaborative Innovation Center of Chemical Engineering & Technology with Environmental Benignity and Effective Resource Utilization, Hunan Provincial Innovation Foundation For Postgraduate (CX2017B333).

REFERENCES

(1) Kuimova, M. K.; Botchway, S. W.; Parker, A. W.; Balaz, M.; Collins, H. A.; Anderson, H. L.; Suhling, K.; Ogilby, P. R. *Nat. Chem.* **2009**, *1*, 69-73.

(2) Luby-Phelps, K. *Curr. Opin. Cell. Biol.* **1994**, *6*, 3-9.

(3) Minton, A. P. *J. Biol. Chem*. **2001**, *276*, 10577-10580.

(4) Ow, Y. P.; Green, D. R.; Hao, Z.; Mak, T. W. *Nat. Rev. Mol. Cell. Biol.* **2008**, *9*, 532-542.

(5) Luby-Phelps, K. *Int. Rev. Cytol.* **1999**, *192*, 189-221.

(6) Olson, K. R.; Dombkowski, R. A.; Russell, M. J.; Doellman, M. M.; Head, S. K.; Whitfield, N. L; Madden, J. A. *J. Exp. Biol.* **2006**, *209*, 4011-4023.

(7) Papapetropoulos, A.; Pyriochou, A.; Altaany, Z.; Yang, G.; Marazioti, A.; Zhou, Z.; Jeschke, M. G.; Branski, L.K.; Herndon, D.N.; Wang, R.; Szabó, C. *Proc. Natl. Acad. Sci. U. S. A.* **2009**, *106*, 21972-21977.

(8) Yang, G.; Wu, L.; Wang, R. *FASEB J.* **2006**, *20*, 553-555.

(9) Zanardo, R. C. O.; Brancaleone, V.; Distrutti, E.; Fiorucci, S.; Cirino, G.; Wallace, J.L. *FASEB J.* **2006**, *20*, 2118-2120.

(10) Abe, K.; Kimura, H. *J. Neurosci*. **1996**, *16*, 1066-1071.

(11) Fu, M.; Zhang, W.; Wu, L.; Yang, G.; Li, H.; Wang, R. *Proc. Natl. Acad. Sci. U. S. A*. **2012**, *109*, 2943-8.

(12) Guo, W.; Kan, J.; Cheng, Z. Chen, J.; Shen, Y.; Xu, J.; Wu, D.; Zhu, Y. *Oxid. Med. Cell. Longev.* **2012**, *2012*,1-9.

(13) Kimura, Y.; Goto, Y.; Kimura, H. *Antioxid. Redox. Signal.* **2010**, *12*, 1-13.

(14) Cheng, W. Y.; Tong, H.; Miller, E. W.; Chang, C. J.; Remington, J.; Zucker, R. M.; Bromberg, P. A.; Samet, J. M.; Hofer, T. P. J. *Environ. Health. Perspect.* **2010**, *118*, 902-908.

(15) Pun, P. B.; Lu, J.; Kan, E. M.; Moochhala, S. *Mitochondrion* **2010**, *10*, 83-93.

(16) Xuan, A.; Long, D.; Li, J.; Ji, W.; Meng, Z.; Hong, L.; Liu, L. *J. Neuroinflammation*. **2012**, *9*, 1-11.

(17) Eto, K.; Asada, T.; Arima, K.; Makifuchi, T.; Kimura, H. *Biochem. Biophys. Res. Commun.* **2002**, *293*, 1485-1488.

(18) Aleardi, A. M.; Benard, G.; Augereau, O.; Malgat, M.; Talbot, J C.; Mazat, J. P.; Letellier, T.; Dachary-Prigent, J.; Solaini, G. C.; Rossignol, R. *J. Bioenerg. Biomembr*. **2005**, *37*, 207-225.

(19) Mecocci, P.; Beal, M.F.; Cecchetti, R.; Polidori, M. C.; Cherubini, A.; Chionne, F.; Avellini, L.; Romano, G.; Senin, U. *Mol. Chem. Neuropathol.* **1997**, *31*, 53-64.

(20) Moreira, P. I.; Cardoso, S. M.; Santos, M. S.; Oliveira, C. R. *J. Alzheimers. Dis*. **2006**, *9*, 101-110.

(21) Jiao, X.; Li, Y.; Niu, J.; Xie, X.; Wang, X.; Tang, B. *Anal. Chem.* **2017**, *90*, 533-555.

(22) Li, X.; Gao, X.; Shi, W.; Ma, H. *Chem. Rev*. **2014**, *114*, 590-659.

(23) Gao, M.; Yu, F.; Lv, C.; Choo, J.; Chen, L. *Chem. Soc. Rev*. **2017**, *46*, 2237-2271.

(24) Zeng, L.; Xia, T.; Hu, W.; Chen, S.; Chi, S.; Lei, Y.; Liu, Z. *Anal. Chem.* **2018**, *90*, 1317-1324.

(25) Mao, Z.; Jiang, H.; Song, X.; Hu, W.; Liu, Z. *Anal. Chem.* **2017**, *89*, 9620-9624.

(26) Feng, W.; Li, M.; Sun, Y.; Feng, G. *Anal. Chem*. **2017**, *89*, 6106-6112.

(27) Liu, H. W.; Li, K.; Hu, X. X.; Zhu, L.; Rong, Q.; Liu, Y.; Zhang, X. B.; Hasserodt, J.; Qu, F. L.; Tan, W. *Angew. Chem*. **2017**, *129*, 11950-11954.

(28) Feng, S.; Liu, D.; Feng, W.; Feng, G. *Anal. Chem*. **2017**, *89*, 3754-3760.

(29) Ou-Yang, J.; Jiang, W. L.; Tan, K. Y.; Liu, H. W.; Li, S. J.; Liu, J.; Li, Y. F.; Li, C. Y. *Sens Actuators B Chem* **2018**, *260*, 264-273.

(30) Yang, Z.; He, Y.; Lee, J. H.; Park, N.; Suh, M.; Chae, W. S.; Cao, J.; Peng, X.; Jung, H.; Kang, H.; Kim, S. J. *J. Am. Chem. Soc.* **2013**, *135*, 9181-9185.

(31) Jiang, N.; Fan, J.; Zhang, S.; Wu, T.; Wang, J.; Gao, P.; Qu, J.; Zhou, F.; Peng, X. *Sens Actuators B Chem* **2014**, *190*, 685-693.

(32) Baek, Y.; Sang, J. P.; Xin, Z.; Kim, G.; Kim, H. M.; Yoon, J. *Biosens.Bioelectron*. **2016**, *86*, 885-891.

(33) Wu, Z.; Liang, D.; Tang, X. *Anal. Chem.* **2016**, *88*, 9213-9218.

(34) Chen, Y.; Zhu, C.; Yang, Z.; Chen, J.; He, Y.; Jiao, Y.; He, W.; Qiu, L.; Cen, J.; Guo, Z. *Angew. Chem. Int. Ed.* **2013**, *52*, 1688-1691.

(35) Pak, Y.; Li, J.; Ko, K. C.; Kim, G.; Jin, Y. L.; Yoon, J. *Anal. Chem.* **2016**, *88*, 5476.

(36) Mao, G. J.; Wei, T. T.; Wang, X. X.; Huan, S. Y.; Lu, D. Q.; Zhang, J.; Zhang, X. B.; Tan, W.; Shen, G. L.; Yu. R. Q. *Anal. Chem*. **2013**, *85*, 7875-7881

(37) Kolanowski, J. L.; Liu, F. New, E. J. *Chem. Soc. Rev.* **2018**, *47*, 195-208.

(38) Dou, K.; Fu, Q.; Chen, G.; Yu, F.; Liu, Y.; Cao, Z.; Li, G.; Zhao, X.; Xia, L.; Chen, G.; Wang, H.; You, J. *Biomaterials* **2017**, *133*, 82-93.

(39) Chen, W.; Pacheco, A.; Takano, Y.; Day, J. J.; Hanaoka, K.; Xian, M. *Angew. Chem. Int. Ed*. **2016**, *55*, 9993-9996.

(40) Zhang, R.; Zhao, J.; Han, G.; Liu, Z.; Liu, C.; Zhang, C.; Liu, B.; Jiang, C.; Liu, R.; Zhao, T.; Han, M. H.; Zhang, Z. *J. Am. Chem. Soc.* **2016**, *138*, 3769-3778.

(41) Guo, B.; Jing, J.; Nie, L.; Xin, F.; Gao, C.; Yang, W; Zhang, X. *J. Mater. Chem. B*. **2018**, *6*, 580-585.

(42) Yan, H.; Yu, F.; Wang, J.; Chen, L. *Anal. Chem*. **2016**, *88*, 4122-4129.

(43) Wang, Y. W.; Liu, S. B.; Ling, W. J.; Peng, Y. *Chem. Commun*. **2016**, *52*, 827-830.

(44) Wang, Y. W.; Hua, Y. X.; Wu, H. H.; Sun, X.; Peng, Y. *Chin. Chem. Lett*. **2017**, *28*, 1994-1996.

(45) Zhang, P.; Li, J.; Li, B.; Xu, J.; Zeng, F.; Lv, J.; Wu, S. *Chem. Commun*. **2015**, *51*, 4414-4416.

(46) Yi, L.; Wei, L.; Wang, R.; Zhang, C.; Zhang, J.; Tan, T.; Xi, Z. *Chem. Eur. J*. **2015**, *21*, 15167-15172.

(47) Hansson, M. J.; Morota, S.; Teilum, M.; Mattiasson, G.; Uchino, H.; Elmer, E.´ *J. Biol. Chem*. **2010**, *285*, 741-750.

(48) Sun, Q.; Collins, R.; Huang, S.; Holmberg-Schiavone, L.; Anand, G. S.; Tan, C. H.; van-den-Berg, S.; Deng, L. W.; Moore, P. K.; Karlberg, T.; Sivaraman. J. *J. Biol Chem*. **2009**, *284*, 3076-3085.

(49) Singh, S.; Padovani, D.; Leslie, R. A.; Chiku, T.; Banerjee, R. *J. Biol. Chem*. **2009**, *284*, 22457-22466.

(50) Feng, W.; Mao, Z.; Liu, L.; Liu, Z. *Talanta* **2017**, *167*, 134-142.

for TOC only